

Ensuring Optimum Solution Circulation in 100% Solar-Powered Absorption Refrigerators

Onochie, E. U.

Department of Mechanical Engineering Technology,
Auchi Polytechnic, Auchi.
Auchi. Edo State, Nigeria.

Ajuwa, C. I.

Department of Mechanical Engineering,
Federal University of Petroleum Resources,
Effurun. Delta State, Nigeria.

Ighodalo, O. A.

Department of Mechanical Engineering,
Ambrose Alli University,
Ekpmoma. Edo State, Nigeria.

Abstract- A standard vapour absorption refrigeration system has a solution pump that transfers solution from the absorber to the generator. Solar energy derived from untraced flat plate solar collectors is adequate for generating refrigerant vapour from refrigerant-absorbent solutions but grossly inadequate for powering a mechanical solution pump. This paper presents the experimental investigation and performance tests of thermal bubble pumps used for lifting the refrigerant-absorbent solution in a 100% solar powered diffusion-absorption refrigerator (DAR) from the generator to the separator, leaving gravity circulation to complete the refrigeration cycle. An experimental rig charged with Methanol was built and set up to test the performance of different bubble pump configurations using real time solar energy collected by two modules of flat plate solar collectors, each having an aperture area of $1m^2$. Measurements of flow rates and temperatures were carried out at operating vacuum pressures and results were analyzed. Experimental results show that a riser diameter of 8mm, submergence ratio of 0.2 and a head of 800mm gave the optimum solution delivery. The DAR is proposed for the preservation of vaccines, fruits and vegetables in farms and rural dwellings where conventional electric power is either scarce or unreliable.

Keywords: *Diffusion-absorption refrigeration; solar energy; submergence ratio; bubble pump; Methanol; Vacuum pressures; flat-plate solar collectors.*

I. INTRODUCTION

Clean energy is now the focus of contemporary technology and researchers are increasingly focusing on renewable energy sources, particularly solar energy. Among all the environmentally friendly and naturally available sources, solar energy stands out on the list of renewable energy sources [1]. There are plenty of technologies currently available to harness the sun's power for heating, cooking, power generation, food drying and refrigeration [2]. Solar energy can provide cheap and clean energy for cooling and refrigeration applications [3]. Preservation of vaccines and perishable agricultural produce is a challenge in rural communities in Edo State,

Nigeria, where electricity is unreliable or sometimes unavailable. Here, solar refrigeration is seen as a veritable alternative to conventional refrigeration driven by electricity and fossil fuels, whose reliability and availability are in doubt. Research work in progress in Auchi, Edo State, is aimed at developing a 100% solar powered vapor absorption refrigerator for rural applications. The major challenge in this project is that of ensuring adequate solution circulation in a continuous vapor absorption refrigeration system devoid of mechanical pumps. The problem is addressed by paying a special attention to the design and selection of the generator-bubble pump-separator assembly in the solar powered diffusion-absorption refrigeration system.

A. Bubble Pump technologies

A standard vapour absorption refrigeration system has a mechanical solution pump that transfers solution from the absorber to the generator. Solar energy, derivable from flat plate solar collectors, is adequate for generating refrigerant vapour from refrigerant-absorbent solutions but grossly inadequate for powering a mechanical solution pump, [4]. The solar powered diffusion-absorption cycle relies on a bubble pump to pump the solution from the generator (boiler) to an appreciable level in a separator, from where gravity circulation completes the cycle. A bubble pump is a fluid pump that operates with thermal energy to pump liquid from a lower level to a higher level. It does not contain any moving parts. The bubble pump operates on the same principle that lifts coffee to the top of the coffee percolator. The bubble pump, as shown in Fig.1, is nothing but a vertical tube of small circular cross-sectional area. The liquid in the reservoir initially fills the tube to the same level (h). Heat is applied at the bottom of the tube at a rate sufficient to evaporate some of the liquid in the tube. The resulting bubbles rise in the tube. Due to the small diameter of the pump tube, the bubbles occupy complete cross-section of the tube and are separated by small liquid slugs. Each bubble

acts as a gas piston and lifts the corresponding liquid slug to the top of the pump tube. The bulk density of the liquid and vapor mixture in the pump tube is reduced relative to the liquid in the liquid reservoir, thereby creating an overall buoyancy lift.

The important parameters of the bubble pump are pump tube diameter (d), driving head (h), pump lift (L) and pump heat input (Q_g). The main characteristic values used to judge the performance of the bubble pump are solution flow rates and the pumping ratio.

Bubble pumps are also known as vapor lift pumps. While commonly used, literature on bubble pumps is not common. However, since a bubble pump is just a pipe containing two-phase fluid flow, books and papers on two-phase flow provide more than sufficient information for the analysis of a bubble pump.

In diffusion-absorption cycles, the bubble pump provides the motive force and is a critical component of the absorption-diffusion refrigeration unit. The performance of the diffusion-absorption cycles depends primarily on the efficiency of the bubble pump [5].

The disadvantage of heat driven bubble pump systems is a very low COP. Therefore, the configuration of the generator, bubble pump and separator is of great importance. In order to increase the COP, it must utilize minimum heat and desorb as much refrigerant as possible from the solution [6]. The bubble pump operates most efficiently in the slug flow regime in which the bubbles are approximately the diameter of the tube. The important parameters of the bubble pump are: pump tube diameter (d), driving head (h), pump lift (L), submergence ratio ($r = h/L$) and pump heat input (Q).

The bubble pump can be driven directly or indirectly by solar energy. The directly driven bubble pump of Diffusion Absorption Refrigerators (DAR) usually consists of a single lifting tube where the heat input is restricted to a small heating

zone by a heating cartridge or the flame of a gas burner with a high heat flux density. The indirectly driven bubble pump consists, on the other hand, of a bundle of tubes as bubble pump, where the heating zone is spread and lower heat flux densities are reached. Here, a secondary heat transfer fluid is used to transfer heat energy from the solar collector array to the generator and then thermal storage tank.

The essential function of the generator is to produce vapor, because it defines the amount of condensate, which is necessary to achieve the cooling capacity of the refrigerator. The production of more refrigerant vapor is obtained by raising the generator temperature.

B. Modeling of a bubble pump.

Reference [7] modelled the bubble pump using simple analytical equations such as Bernoulli's equation, the Continuity equation, mass balance, the momentum conservation equation and necessary simplifying assumptions. The theoretical prediction of the performance of the bubble pump so obtained is compared with the empirical results and a correlation established.

A bubble pump operates most efficiently in the slug flow regime. The maximum diameter tube in which slug flow occurs is given by the following equation [8]:

$$d \leq 19. \sqrt{\left(\frac{\sigma \cdot v_f}{g \left(1 - \frac{v_f}{v_g} \right)} \right)}$$

(1) Where v_f and v_g are the specific volumes of the liquid and vapor respectively, and σ is the surface tension.

Note, for a given fluid in a tube of diameter greater than that predicted by the above equation, slug flow will never occur.

In carrying out a theoretical modeling of the bubble pump, simple analytical equations like the Bernoulli's equation, continuity equation, momentum equation, boiling and condensation heat transfer phenomena were useful.

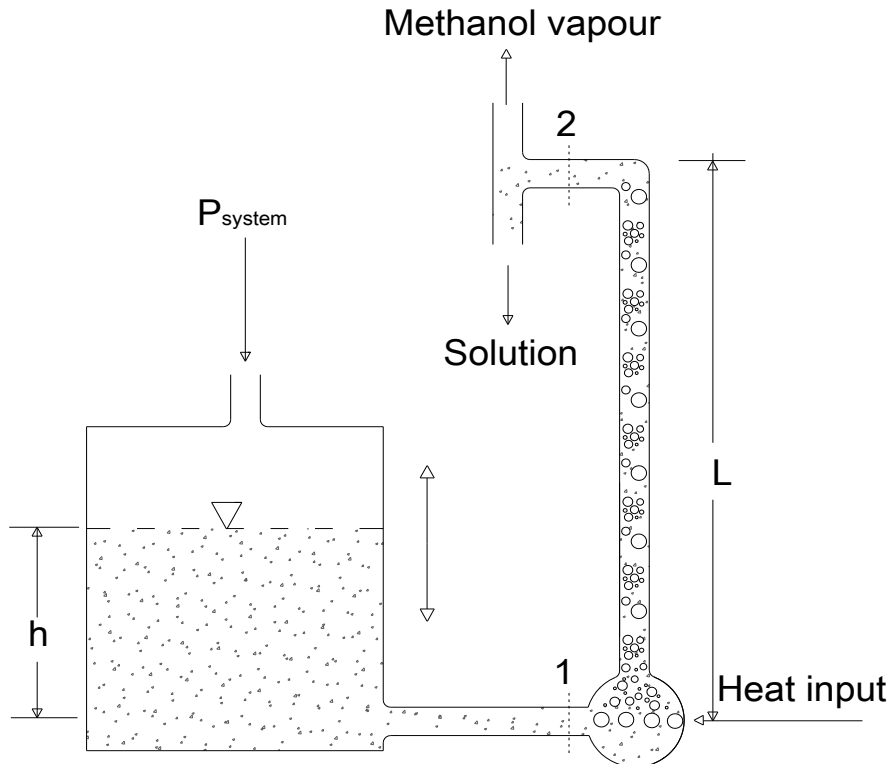


Fig. 1. Schematic diagram of a bubble pump

In Fig. 1, Point 1 represents the inlet of the bubble pump.

Applying Bernoulli's equation

between the surface of reservoir and Point 1 yields:

$$P_1 + \rho_1 \cdot g \cdot h + \rho_1 \cdot \frac{V_1^2}{2} = P_{system} \quad \text{or} \quad P_{system} = P_1 + \rho_1 \cdot (g \cdot h + \frac{V_1^2}{2}) \quad (2)$$

Next, the continuity equation is applied to the control volume (CV) into which heat is applied. Assuming that the mixture of vapour bubbles and the liquid exit this control volume at a mixture velocity, V_2 , the continuity equation yields:

$$\dot{m}_2 = \dot{m}_1 \quad (3)$$

$$\text{Or} \quad \frac{A \cdot V_2}{v_2} = \frac{A \cdot V_1}{v_1} \quad (4)$$

Rearranging the terms, and noting that $A_1 = A_2 = A$, we have

$$V_2 = \frac{v_2 \cdot V_1}{v_1} \quad (5)$$

The specific volume at Point 2, v_2 is assumed to be the specific volume of a vapour-liquid mixture with a quality x .

$$v_2 \text{ can then be expressed as } v_2 = v_f + x \cdot (v_g - v_f) = v_f \left(1 + x \left(\frac{v_g - v_f}{v_f} \right) \right) \quad (6)$$

$$\text{Where } x = \frac{\dot{m}_g}{\dot{m}_f + \dot{m}_g} \quad (7)$$

Combining equation (5), (6), and (7)

$$V_2 = V_1 \cdot \frac{v_f}{v_1} \left(1 + \left(\frac{\dot{m}_g}{\dot{m}_f + \dot{m}_g} \right) \left(\frac{v_g - v_f}{v_f} \right) \right) \quad (8)$$

Now, if the mass flow rate of the liquid is assumed negligible relative to the mass flow rate of vapour and the specific volume of the liquid is assumed negligible relative to the specific volume of the vapour, equation (8) becomes:-

$$V_2 = V_1 \cdot \frac{v_f}{v_1} \cdot \left(1 + \frac{\tilde{V}_g}{\tilde{V}_f}\right) \quad (9)$$

Where $\dot{m}_g \cdot v_g = \tilde{V}_g$ and $\dot{m}_f \cdot v_f = \tilde{V}_f$

Next, neglecting the friction drop over the tube length in (Fig 1), the rate of change of linear momentum across the control volume can be written as

$$\rho_2 \cdot A \cdot V_2 \cdot V_2 - \rho_1 \cdot A \cdot V_1 \cdot V_1 = (P_2 - P_1) \cdot A \quad (10)$$

But from conservation of mass,

$$\rho_2 \cdot A \cdot V_2 = \rho_1 \cdot A \cdot V_1 \quad (11)$$

Combining equation (10) and (11), we have

$$\rho_1 \cdot V_1 (V_2 - V_1) = (P_2 - P_1) \quad (12)$$

Substituting equation (9) into equation (12), we have

$$\begin{aligned} P_2 &= P_1 + \rho_1 \cdot V_1 \cdot \left(V_1 \cdot \frac{v_f}{v_1} \cdot \left(1 + \frac{\tilde{V}_g}{\tilde{V}_f}\right) - V_1 \right) \\ &= P_{system} - \rho_1 \cdot \left(g \cdot h + \frac{v_1^2}{2} \right) + \rho_1 \cdot V_1^2 \cdot \left(\left(1 + \frac{\tilde{V}_g}{\tilde{V}_f}\right) - 1 \right) \\ P_2 &= P_1 + \rho_1 \cdot V_1^2 \cdot \left(\left(1 + \frac{\tilde{V}_g}{\tilde{V}_f}\right) - 1 \right) \\ P_2 &= P_1 + \rho_1 \cdot V_1^2 \cdot \left(\left(1 + \frac{\tilde{V}_g}{\tilde{V}_f}\right) - 1 \right) \quad (13) \end{aligned}$$

Since $v_1 = v_f$ from Fig. 1 and from equation (2)

$$P_{system} = P_1 + \rho_1 \cdot \left(g \cdot h + \frac{v_1^2}{2} \right), \text{ or}$$

$$P_1 = P_{system} - \rho_1 \cdot \left(g \cdot h + \frac{v_1^2}{2} \right) \quad (14)$$

Substituting equation (14) into equation (13),

$$P_2 = P_{system} - \rho_1 \cdot g \cdot h + \rho_1 \cdot \frac{v_1^2}{2} + \rho_1 \cdot V_1^2 \cdot \left(\frac{\tilde{V}_g}{\tilde{V}_f} \right) \quad (15)$$

Now, applying the conservation of momentum to the bubble pump tube connecting the generator and the separator,

$$P_2 - P_{system} = \frac{1}{2} \cdot f \cdot \rho_f \cdot V_2^2 \cdot \left(\frac{L \cdot B}{A} \right) + \frac{W}{A} \quad (16)$$

Where B is the perimeter of the bubble pump tube and W is the weight of fluid in the bubble pump tube. The weight (W) can be expressed as the combined weight of the liquid and vapour in the tube.

$$W = L \cdot g \cdot (\rho_f \cdot A_f + \rho_g \cdot A_g) \quad (17)$$

Where A_f is the superficial area through which the liquid flows and A_g is the superficial area through which the vapour flows. Equation (17) is simplified by assuming that the density of the vapour phase is negligible as compared to that of the liquid.

$$W = L \cdot g \cdot \rho_f \cdot A_f \quad (18)$$

We can also write down the following equations for volume flow rates of liquid and gas thus:-

$$\tilde{V}_f = A_f \cdot V_f \quad (19)$$

$$\tilde{V}_g = A_g \cdot V_g \quad (20)$$

$$A = A_f + A_g \quad (21)$$

Using these equations,

$$\frac{W}{A} = \frac{L \cdot g \cdot \rho_f \cdot A_f}{A_f + A_g} = \frac{L \cdot g \cdot \rho_f}{1 + \frac{A_g}{A_f}} \quad (22)$$

$$\frac{W}{A} = \frac{L \cdot g \cdot \rho_f}{1 + \left(\frac{\tilde{V}_g}{\tilde{V}_f} \cdot s \right)}, \quad (23)$$

Where s is defined as the flow rate ratio between the vapour and liquid, i.e. $s = V_g/V_f$

Substituting equation (23) into equation (16), we have

$$P_2 - P_{system} = \frac{1}{2} \cdot f \cdot \rho_f \cdot V_2^2 \cdot \left(\frac{L \cdot B}{A} \right) + \frac{L \cdot g \cdot \rho_f}{1 + \left(\frac{\tilde{V}_g}{\tilde{V}_f} \cdot s \right)} \quad (24)$$

Now substituting equation (9) into equation (24),

$$P_2 = P_{system} + \frac{f \cdot L}{d} \cdot \frac{\rho_f \cdot V_1^2}{2} \cdot \left(1 + \frac{\tilde{V}_g}{\tilde{V}_f} \right)^2 + \frac{L \cdot g \cdot \rho_f}{1 + \left(\frac{\tilde{V}_g}{\tilde{V}_f} \cdot s \right)}, \quad (25)$$

Noting that ratio of area to perimeter $\frac{A}{P} = d$

Finally equation (25) is equated with equation (15),

$$\rho_1 \cdot g \cdot h + \rho_1 \cdot V_1^2 \cdot \left(\frac{\tilde{V}_g}{\tilde{V}_f} \right) = \frac{f \cdot L}{d} \cdot \frac{\rho_f \cdot V_1^2}{2} \cdot (1 + \frac{\tilde{V}_g}{\tilde{V}_f})^2 + \frac{L \cdot g \cdot \rho_f}{1 + \left(\frac{\tilde{V}_g}{\tilde{V}_f} \right)^2}, \quad (26)$$

Noting that $\rho_1 = \rho_f$ since $v_1 = v_f$, and dividing all through by $L \cdot g \cdot \rho_f$, we have

$$\begin{aligned} \frac{h}{L} + \frac{1}{\left(1 + \frac{v_g}{v_{f,s}}\right)} &= \frac{V_1^2}{2 \cdot g \cdot L} + \frac{V_1^2}{g \cdot L} \left(\frac{\tilde{V}_g}{\tilde{V}_f} \right) - \frac{f \cdot L}{g \cdot d \cdot L} \cdot \frac{V_1^2}{2} \cdot (1 + \frac{\tilde{V}_g}{\tilde{V}_f})^2 \\ &= \frac{V_1^2}{2 \cdot g \cdot L} \left[1 + 2 \left(\frac{\tilde{V}_g}{\tilde{V}_f} \right) - \frac{f \cdot L}{d} \cdot (1 + \frac{\tilde{V}_g}{\tilde{V}_f})^2 \right] \text{ or} \\ \frac{h}{L} + \frac{1}{\left(1 + \frac{v_g}{v_{f,s}}\right)} &= \frac{V_1^2}{2 \cdot g \cdot L} \cdot 1 + 2 \left[\left(\frac{\tilde{V}_g}{\tilde{V}_f} \right) - \frac{f \cdot L}{d} \cdot (1 + \frac{\tilde{V}_g}{\tilde{V}_f})^2 \right] \quad (27) \end{aligned}$$

where $k = \frac{f \cdot L}{d}$, noting that

f , the laminar friction factor, is calculated assuming only liquid flow throughout the pipe and is given by

$$f = \frac{64}{Re}, \quad (28)$$

Where Re is the Reynold's Number. For tube diameter d ,

$$Re_d = \frac{\rho_1 \cdot V_1 \cdot d}{\mu} \quad (29) \quad k$$

can be an adjusted to account for other losses, in addition to friction losses in the tube. Furthermore, k may also be adjusted to match experimental data since losses are sometimes difficult to quantify analytically.

In the conventional diffusion-absorption refrigeration system, vapour bubbles are produced by the addition of heat to the lower portion of the bubble pump tube. Assuming the fluid in the generator and the tube to be at the saturated temperature and no heat transfer over the length of the pump tube, heating power required to produce the desired vapour flow rate is,

$$Q_{vap} = \rho_g \tilde{V}_g h_{fg} \quad (30)$$

assuming that the working fluid is at saturated temperature and the specific enthalpy

$$h_{fg} = h_g - h_f.$$

The amount of liquid pumped can be expressed as

$$\dot{m}_f = \rho_f \cdot \tilde{V}_f = \rho_f \cdot V_1 \cdot A \quad (31)$$

Where V_1 is the velocity at the entrance to the bubble pump at point 1.

Dividing equation (30) by equation (31) gives the relationship between the heat input and the pumping ratio, $r_p = \tilde{V}_g / \tilde{V}_f$, thus

$$Q_{vap} / \dot{m}_f = \rho_g \tilde{V}_g h_{fg} / \rho_f \cdot \tilde{V}_f \quad (32)$$

Equation (27) gives the relationship between the submergence ratio $r = h/L$, the pumping ratio $\tilde{V}_g / \tilde{V}_f$ and the diameter of the pump tube given by $k = \frac{f \cdot L}{d}$.

Thus, all the bubble pump parameters can be estimated from the mathematical modeling and predictions compared with experimental results.

II. METHODOLOGY

The methodology includes the design and construction of an experimental rig used to evaluate the performance of several configurations of bubble pumps adaptable to solar refrigeration systems working with methanol as refrigerant. Since the object is to investigate the relationship between the flow rates of the working fluids and the heat input for varying pump diameters and submergence ratios, the evaporator and absorber are excluded in the experimental rig. The flow diagram of the experimental rig showing the relevant components and their relative positions is therefore as shown in Fig 2.

The experimental rig consists of two modules of flat plate solar collectors, thermal storage tank, generator-bubble pump-separator assembly, condenser, receiver and instrumentation for measuring flow rates, temperature and pressure. The design and construction of the components were carried out as follows:-

The relationship between flow rates of the working fluids namely methanol vapor, estimated by the Methanol condensate coming from the condenser and the methanol – bromide solution, the rates of heat input for varying pump tube diameters and submergence ratios, is investigated using real time solar heat flux collected from two modules of flat plate solar collectors and also electrically simulated solar energy. The empirical results obtained experimentally were compared with results predicted theoretically and a correlation determined.

A. The flat plate solar collectors.

The average daily solar radiation at the upper limits of the atmosphere at Auchi, Edo State, ($7^{\circ} 4'N$, $6^{\circ}16'E$) is estimated to be 0.7254 KW/m^2 [9,10]. Assuming that about 50% of this radiation is lost due to the cloudiness of the atmosphere and a further 10% due to the inefficiency of the solar collectors, the net average solar energy available for driving the bubble pump of the solar absorption refrigerator is approximately 0.29 KW/m^2 . Choosing a total collector aperture area of 2.0 m^2 corresponding to two flat plate solar collector modules, each having an aperture area of 1m^2 , the estimated solar heat power available for driving the absorption refrigerator is 0.58 KW .

The solar collector tilt is adjustable but fixed at 7° to the horizontal. This angle corresponds to the latitude of Auchi. The collector modules are positioned to face due south. The tilt improved the solar heat power collected and also sustained thermo-siphon circulation of the heat transfer fluid in the collectors.

The collector tubes and plates are constructed with aluminum. The absorber plates are insulated at the base with Poly-Urethane-Foam, packed inside a box made of aluminum sections and covered with 10mm thick window glass. The absorber plates of the collector modules are painted matt black.

B The thermal storage tank

The thermal storage tank is constructed from 200mm diameter stainless steel cylinder of height 1m. This has a capacity of about 0.0314 m^3 or 31.4 litres. The heat transfer fluid, water doped with 20% ethylene glycol, flows from the solar collector modules to the thermal storage tank through the generator, and back to the collectors by thermo-siphon circulation. The thermal storage tank is well lagged to reduce heat loss to the atmosphere.

C. The generator-bubble pump-separator assembly.

The major challenge in the design and construction of the generator-bubble pump-separator assembly is the difficulty in achieving a leak-proof construction because of the numerous joints. The assembly was first constructed with high pressure PVC pipes and 10mm Perspex sheet but the glued joints failed under pressure. Next, the components were constructed from stainless steel but the imperfection in stainless steel welding resulting in tiny pin holes at joints led to leakage and loss of vacuum. Finally,

an all copper construction gave a better result due to a better joining technique by copper brazing.

The generator housed a 2-pass copper tubing of diameter 19mm through which the solar heated water passed to reach the thermal storage tank. Multiple riser bubble pump tubes rose from the generator to the separator. The pump tubes penetrated the separator so that the solution is spewed into the separator in the form of a fountain. A liquid level monitor on the adjustable receiver enabled the level of solution in the pump tubes to be monitored. There is a provision to pipe away the methanol vapour to the condenser and to conduct the solution collected in the separator to the receiver.

Four sets of generator-bubble pump-separator assembly with tube diameters 6mm, 8mm, 10mm and 12mm were produced with provisions for varying the lengths of pump tubes. Each installation was pressure tested for leakage, evacuated and charged with Methanol solution before experiments were conducted.

D. The condenser

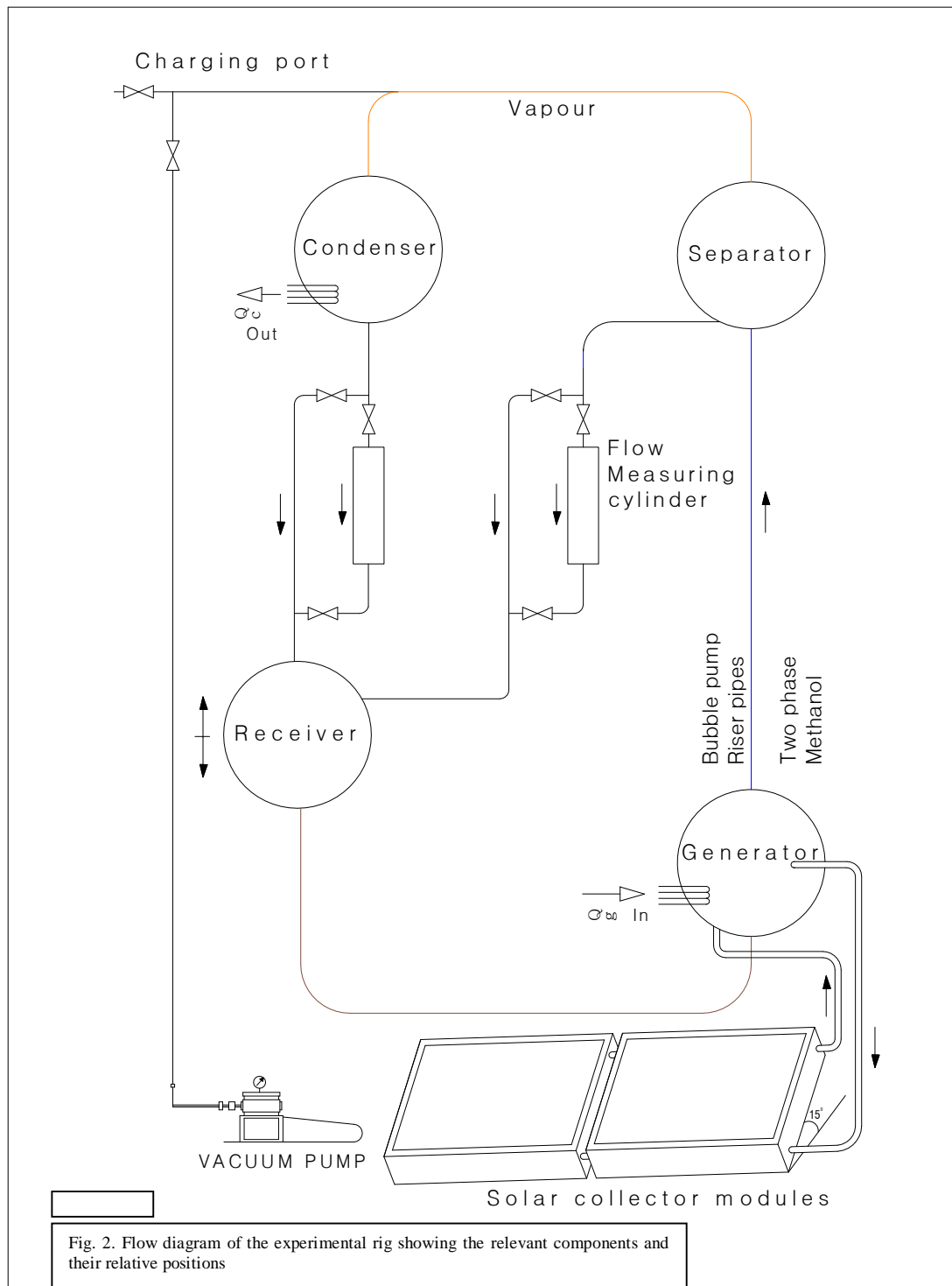
The condenser collects vapour from the separator and condenses it to liquid methanol by rejecting heat to the cooling water from the cooling water header tank. The condenser is constructed from a 100mm copper cylinder with in-built copper cooling coils.

E. The receiver

The receiver receives both the solution from the separator and the methanol condensate from the condenser. The condensate dilutes the solution from the separator before it is fed to the generator. The receiver is provided with a mechanism to adjust its level in order to raise or lower the driving head, h , thus varying the submergence ratio, h/L . The receiver too is constructed from the 100mm copper cylinder and has the charging valve and compound pressure gauge connected to it.

F. Instrumentation for data acquisition.

A vacuum pump is installed to the experimental rig as indicated in Fig.2. A compound pressure gauge is connected to the receiver for monitoring the evacuation process and the operating pressures. Thermometer wells are provided at the inlet and outlet to the generator, and also at the top of the thermal storage tank for monitoring the temperatures with digital thermometers. Flow rate



meters that would not add to the flow resistance or obstruct flow are installed between the separator and the receiver, and between the condenser and the receiver. Transparent flexible tubes with a set of controlling valves as indicated

in Fig. 2 are incorporated as ballistic cylinders. A stopwatch is used with the ballistic cylinders in measuring flow rates of the working fluids.

G. Experimental set-up

The generator-bubble pump-separator assembly is of 16 variants - each of the four assemblies with different diameters, i.e. 6mm, 8mm, 10mm and 12mm, is varied in lengths of 0.6m, 0.8m, 1.0m and 1.2m. When one particular configuration is installed, it is completely evacuated and tested for leakage over a long period before running the experiments. Heat energy is added to the system in two alternate ways- by electrical simulation of solar heat and by real time solar heat energy from two modules of flat plate solar collectors. After set-up and evacuation, the rig is charged with methanol- Lithium Bromide solution. The experimental rig is borne on a stable Dixon-iron framework

III. RESULTS AND DISCUSSION

Typical results obtained on clear days from the experimental rig are as depicted in Tables 1 & 2 and figures 3 & 4 below;-Solar collector energy output in W/m^2 is proportional to the temperature difference between the inlet and outlet ports of the generator. The temperature difference therefore serves as a good estimate of the heat input into the generator. Collector energy output Q_c in W/m^2 is given by

$$Q_c = \alpha (t_i - t_o) = \alpha t_d.$$

Where t_d is temperature difference in $^{\circ}\text{C}$

From pressure, temperature and flow rate measurements taken every hour, from 6am to 6pm, the average regeneration temperature obtained on a typical clear day, between 10am and 3pm was 60°C . The corresponding lowest evaporator temperature obtained from the experimental solar refrigerator was 7°C .at a Heat Ratio, ε_{TH} (Equivalent Coefficient of Performance, COP, of an absorption refrigeration system) estimated at 0.58, thus:-

ε_{TH} = refrigerating capacity/energy collected, at peak performance.

$$= \dot{m}_c \cdot C_p \cdot (t_a - t_e) / I_c$$

Where \dot{m}_c = Density, $\rho_c \text{ Mol/l} \times V_1$ (measured average Volume flow rate of methanol condensate from condenser to evaporator = $5.044 \times 10^{-3} \text{ l/s}$)

$$= 24.4 \text{ Mol/l} \times 5.044 \times 10^{-3} \text{ l/s}$$

$$= 1.23 \times 10^{-1} \text{ Mol/s}$$

C_p = Specific heat capacity of methanol condensate at 7°C (280°K) = 78.19 Joules/(Mol. $^{\circ}\text{K}$) (Table 1)

t_a = Ambient temperature outside = 30°C

t_e = Minimum evaporator temperature = 7°C , and

I_c = Estimate of total heat power collected = $0.448 \text{ kW} = 448 \text{ W}$

$$\text{i.e. } \varepsilon_{\text{TH}} = \{ 1.23 \times 10^{-1} \text{ Mol/s} \times 78.19 \text{ Joules/(Mol. } ^{\circ}\text{K}) \times (30-7) ^{\circ}\text{K} \} / 448 \text{ W} \\ = 0.58$$

A. Parameters influencing the performance of bubble pump

The bubble pump operates most efficiently in the slug flow regime in which the bubbles are approximately the diameter of the tube, [11]. Bubble pump tube diameter d , pump lift L , driving head h and heat input Q_i to the bubble pump tube were varied to study the bubble pump performance. There is a maximum tube diameter above which slug flow will not occur, as predicted by Chisholm. The phenomenon predicted by the above correlation has also been observed by experimentation and was found that after a maximum lift-tube diameter has been exceeded, there is a change in the flow pattern from slug flow to an intermittent churn-type flow [12].Excessively large tube diameters caused pumping to stop altogether. Reference [12] found the limiting diameter to be 18 mm. They also found that the frequency of the pumping action was observed to increase with rising heat input Q_i to the bubble pump, increase in driving head h , decrease in pump lift L and reduction in tube diameter d .

Reference [13] found that after a certain pumping height is exceeded, the pumping action stopped and classified this restriction as the discharge limit. They noted that as the lift tube

Table 1; Variation of collector energy output (W/m^2) with solar time for a typical clear day.

Collector output, Q_c vs Solar Time	Temperature $^{\circ}\text{C}$		
	Generator Inlet temperature $t_{in}^{\circ}\text{C}$	Generator Outlet temperature $t_{in}^{\circ}\text{C}$	Temperature difference, t_d $^{\circ}\text{C}$
6:00 am	32	27	5
7:00 am	36	28	8
8:00 am	39	29	10
9:00 am	41	30	11
10:00 am	45	31	14
11:00 am	56	31	25
12:00 am	65	32	33
1:00 pm	72	32	40
2:00 pm	73	33	40
3:00 pm	68	32	36
4:00 pm	63	31	32
5:00 pm	52	30	22

Table 2; Variation of flow rate in Mol/s with heat input for different submergence ratios, r , for a typical clear day.

$\text{W/m}^2 = \alpha(t_i - t_0)$ t_d $^{\circ}\text{C}$	Variation of flow rate of solution in Mol/s with heat input Q_c		
	Flow rate of solution $\times 10^{-1}$ Mol/s for $r = 0.6$	Flow rate of solution $\times 10^{-1}$ Mol/s for $r = 0.4$	Flow rate of solution $\times 10^{-1}$ Mol/s for $r = 0.2$
5	0	0	0
8	0	0	0
10	0	0	0.42
11	0.55	0.72	0.92
14	0.93	1.20	1.52
25	1.36	1.71	2.22
33	1.78	2.25	2.75
40	2.15	2.75	3.43
40	2.25	2.80	3.51
36	2.10	2.50	3.15
32	1.82	2.25	2.82
22	1.55	2.00	2.52

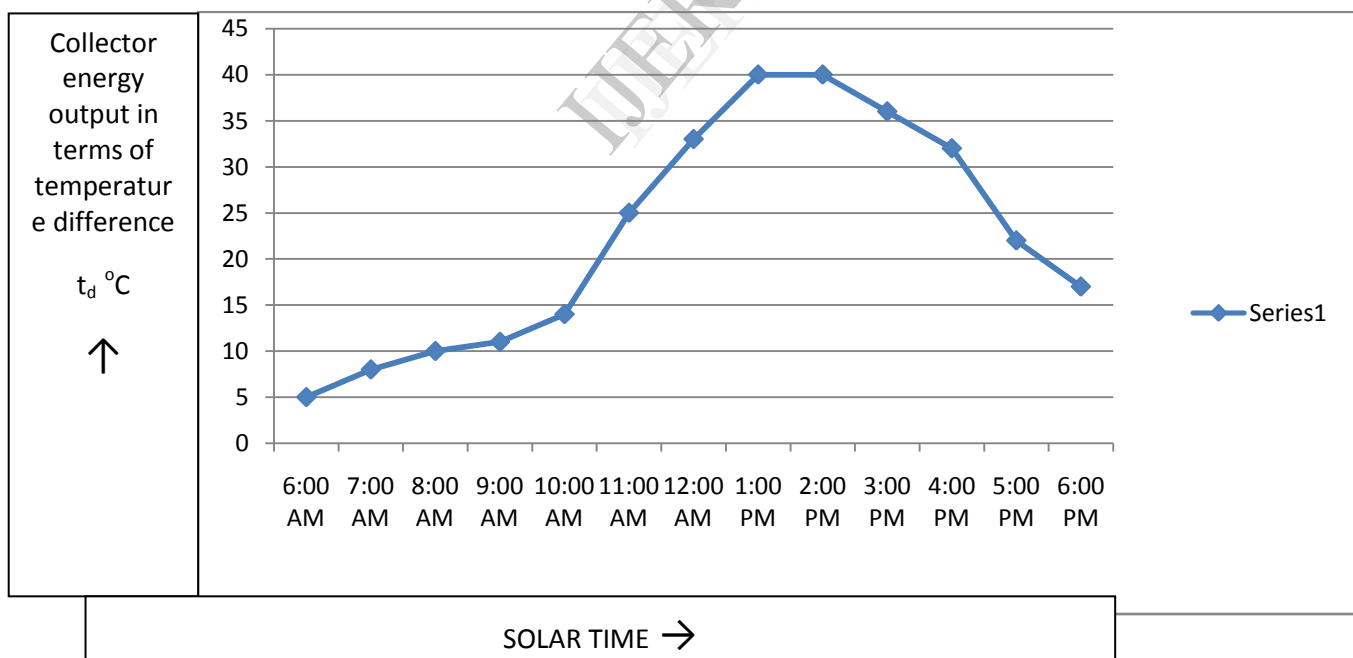


Fig.3: Variation of collector energy output (W/m^2) with solar time for a clear day.

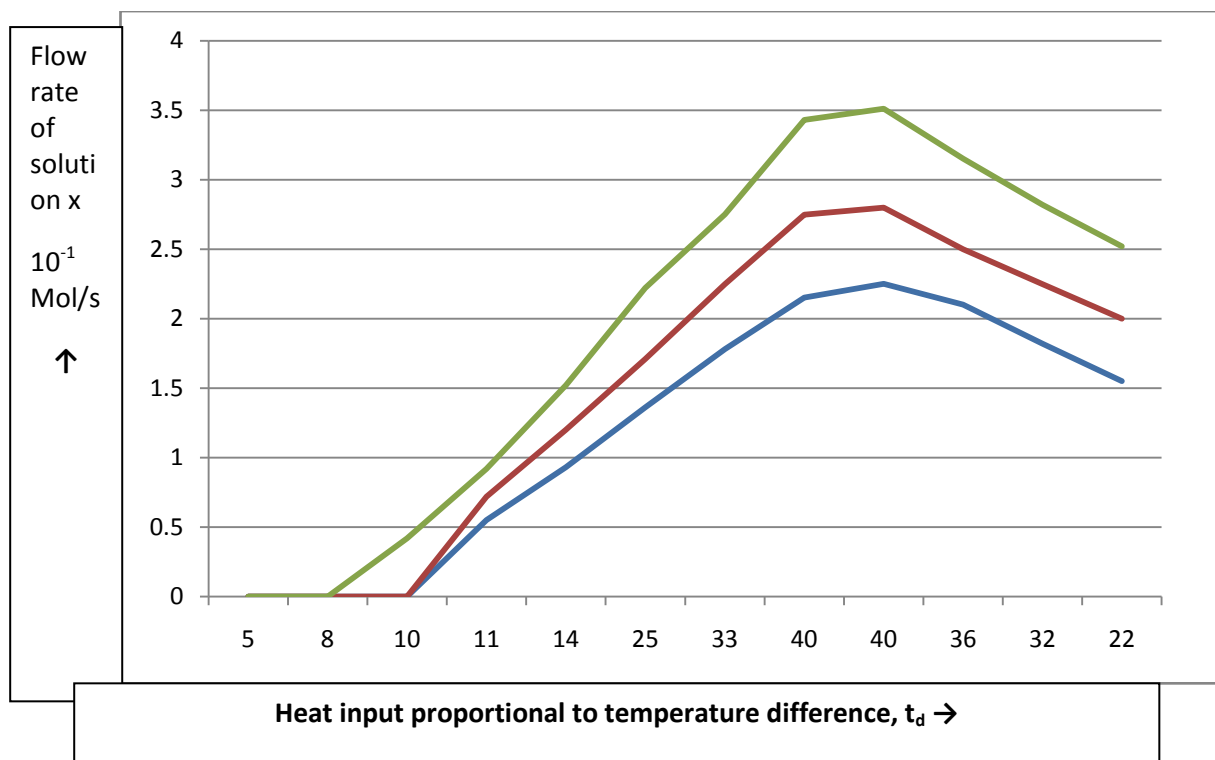


Fig. 4. Variation of solution flow rate with solar heat input for Submergence ratio $r = 0.2, 0.4$ and 0.6

diameter increases the maximum pumping height decreases. This further restricts the diameter of the lift tubes if it is to be used on tall machines. The equation of Chisholm is used by [14] to estimate the pump tube diameter d for the operating conditions chosen.

The Einstein refrigeration cycle was studied extensively in Georgia Institute of Technology where Delano found that increasing the heat input to the bubble pump for a fixed submergence ratio will increase the flow rate of the liquid through the bubble pump to a maximum and then any further increase in the heat input will decrease the liquid flow rate. He showed that increase in the tube diameter would increase the flow rate through the bubble pump since this would decrease the friction factor.

The optimum efficiency diameter occurs while operating in the slug regime, [11]. It is recommended to use a slightly larger diameter than the optimum value. Experiments show that the driving head h is one of the most dominant parameters influencing the bubble pump performance. Changing the driving head by 10% will result in about 40% change in the mass flow rates. It was concluded that a low driving head h given by a submergence ratio of about 0.2 is recommended to achieve higher refrigerant flow rates and thus higher cooling capacity.

IV. CONCLUSION

The results of this work show that the optimum parameters of a bubble pump for improved solution circulation and subsequent adaptation to the diffusion-absorption refrigeration system are pump tube diameter $d = 8\text{mm}$, pump lift $L = 0.8\text{m}$, and submergence ratio $r = 0.2$. This pump configuration is therefore incorporated in the design of an experimental diffusion – absorption refrigerator under development in Auchi, Edo State, Nigeria.

During the course of this work, it is found that:-

- The operating pressures are between 200mbar and 500mbar depending on the heat input. The difference between the condenser and absorber pressures is significant enough to maintain circulation of working fluid. The operating vacuum pressures also mean that low heat energy derivable from solar collectors are sufficient to drive the solar refrigerators due to low saturation temperatures of Methanol at these pressures
- The heat flux when using electrically simulated heat energy is quite greater than that obtained when using real time solar energy collected with flat plate solar collectors. This makes the results obtained by simulation better than those obtained from solar heat driven systems.

- The performance of the bubble pump is best during slug-flow regimes when the diameter of the bubble is approximately that of the bubble pump tube.
- The flow rate increases with increase in pump tube diameter until an optimum diameter is reached. As the diameter is further increased, the flow rate reduced for a given submergence ratio and heat input
- Increasing submergence ratio also resulted in increase in flow rate until the optimum value is reached. After this the flow rate decreased for a given heat input.
- The performance of the bubble pump varies with sun's declination, the time of the day and clearness factor of the sky in response to the solar heat input. There are values of solar heat input when there is no circulation of the working solution. The thermal storage system is meant to act as a back-up for such periods so that circulation will be continuous. It means therefore that the capacity and effectiveness of the thermal storage tank would have to be reviewed.

ACKNOWLEDGMENT

I wish to thank Dr. (Mrs) P. O. Idogho, Rector, Auchi Polytechnic, Auchi and the Tertiary Education Trust Fund (TETfund), Abuja, Nigeria, for partially sponsoring this research work.

REFERENCES

1. H. Z. Hassan, A. A. Mohamad. "A Review on Solar-powered Closed Physio-sorption Cooling Systems". *Renewable and Sustainable Energy Reviews* 2012;16: 2516 -38.
2. H. Z. Hassan, A. A. Mohamad, H. A. Al-Ansary. "Development of a Continuously Operating Solar-driven Adsorption Cooling System: Thermodynamic Analysis and Parametric Study". *Applied Thermal Engineering* 2012; 48:332-41.
3. C. Koroneos, E. Nanaki, G. Xydis. "Solar Air-conditioning Systems and their Applicability —An Exergy Approach". *Resources, Conservation and Recycling* 2010;55:74-82.
4. E. U. Onochie, "Design and Construction of a 100% Solar Powered Continuous Vapour Absorption Refrigerator" presented at the 3rd National Solar Energy Forum, Akoko, Lagos . 1987
5. P. Srikhirin, and S. Aphornratana," Investigation of a Diffusion Absorption Refrigerator". *Applied Thermal Engineering*, 2002; 22: pp 1181-93.
6. A. Zohar, M. Jelinek, A. Levy, and I. Borde, "The Influence of the Generator and Bubble Pump Configuration on the Performance of Diffusion Absorption Refrigeration (DAR) System". *International. Journal of. Refrigeration*, 2008; 31: pp 962-69
7. A.D.Delano. "Design Analysis of the Einstein Refrigeration Cycle." Ph.D. Thesis, Georgia Institute of Technology. Georgia, 1998. (www.me.gatech.edu/energy/andy_phd)
8. D.Chisholm "Two-Phase Flow in Pipelines and Heat Exchangers". 1983; Longmans Inc., New York.
9. J. L.Threkeld. "Thermal Environmental Engineering" 1970; 2nd Ed. Prentice-Hall. Pp 292-94
10. E. U. Onochie. "Computation of Solar Insolation Data Within the Tropics". Presented at the 2nd National conference on Engineering Education, Federal Polytechnic, Mubi. Adamawa State, Nigeria, 1989
11. S.J. White. "Bubble Pump Design and Performance". Ph.D Thesis, Georgia Institute of Technology, Georgia 2001.
12. M. Pfaff , R. Sasavanan, M.P. Maiya and S.S. Murthy." Studies on Bubble Pump for a Water-Lithium Bromide Vapour Absorption Refrigerator". *International Journal of. Refrigeration*,1998; 21: pp 452-62
13. J. Siyetlmg and L.Sang-Kyun, "Pumping Characteristics of a Thermo-siphon Applied for Absorption Refrigerators with Working Pair of LiBr/Water". *Applied Thermal Engineering*. 1998; 18: pp1309-23.
14. U. Jakob, U.Eicker, D. Schneider, and A. Teuüber. "Experimental Investigation of Bubble Pump and System Performance for a Solar Driven 2.5 kW Diffusion Absorption Cooling Machine" *Proceedings of Sustainable Energy Technologies, (HSET '07)*, 2007; Chambery, pp: 789-796.